Molecular Spectra As a Tool in Assigning Carbon 1s Photoelectron Spectra of Physisorbed Overlayers

ARTICLE *in* THE JOURNAL OF PHYSICAL CHEMISTRY C · SEPTEMBER 2010

Impact Factor: 4.77 · DOI: 10.1021/jp1003352

Molecular Spectra As a Tool in Assigning Carbon 1s Photoelectron Spectra of Physisorbed Overlayers

Maria G. Zahl,[†] Velaug Myrseth,[‡] Trine H. Andersen,[§] Jarle Harnes,[†] Anne Borg,[§] Leif J. Sæthre,[†] and Knut J. Børve*,[†]

Department of Chemistry and Department of Physics and Technology, University of Bergen, NO-5020 Bergen, Norway, and Department of Physics, Norwegian University of Science and Technology, NO-7491 Trondheim, Norway

Received: January 13, 2010; Revised Manuscript Received: July 13, 2010

Carbon 1s photoelectron spectra were measured for 1,1-dichloroethene and 1,3-cyclohexadiene adsorbed on Si(111)-7×7 and for gaseous cyclopentene and 1,1-dichloroethene. We explore closely how the molecular spectra of 1,1-dichloroethene and 1,3-cyclohexadiene change upon physisorption and show how gas-phase X-ray photoelectron spectra can be a useful tool for interpretation of spectra of physisorbed molecules. When assigning spectra of adsorbed states, it is frequently assumed that carbon 1s ionization energies (IE) group according to the hybridization state of the carbon atom and, moreover, that sp^3-hybridized carbons have lower ionization energies than do sp^2-hybridized carbons. These assumptions are explored by reviewing gas-phase spectra where it is possible to assign spectral peaks to individual carbon atoms without ambiguity. In cyclopentene, the carbon 1s ionization energies do group according to hybridization, albeit with the sp^3 carbons at higher IE than the sp^2 carbons. In propene, the 1s ionization energy of the central, unsaturated carbon atom groups together with that of the methyl rather than the terminal sp^2 carbon, almost 0.5 eV higher than the IE of the latter. These findings are backed by a sizable data set, showing unequivocally that the practice of assigning spectra based on the assumption that sp^2 carbons appear at higher C1s ionization energies than do sp^3 carbons is unjustified.

Introduction

Adsorption of organic compounds on well-defined surfaces of semiconductors such as Si(100) and Si(111)-7×7, has grown into an important topic of research due to its close connection to further development of microelectronics. Unsaturated carbon compounds are of particular interest since several are found to adsorb readily on silicon and to give rise to ordered overlayers.[1−6] The adsorbing molecules may possess additional functional groups, which allows for the possibility of functionalizing the surface.[7−9]

Although it is the possibility of direct electronic coupling between an organic overlayer and the silicon substrate, i.e., the formation of a chemisorption layer, that is at heart of interest in these systems, they also present interesting challenges with respect to characterizing the adspecies formed. In particular, while a chemisorbed layer may be formed at ambient deposition temperatures, one or several physisorbed overlayers may form on top of that if the sample is dosed at liquid-nitrogen temperatures or below.

By definition,[10] a physisorbed molecule is bonded to the surface by nonspecific van der Waals forces,[11] which implies that the molecular orbitals of the molecule are perturbed only to a small degree. This is in contrast to a chemisorbed adspecies, which is attached to the surface by way of (polar) covalent bonding. While the distinction is in principle clear, many adsorption systems display surface bonds in between these extremes, for instance involving strong hydrogen bonding or weak charge transfer.

An interesting example of the latter is the adsorption of *n*-octane on Cu(110), previously thought to present a classical example of physisorption. However, X-ray emission and absorption experiments in conjunction with theoretical models reveal considerable electron sharing between metal and adsorbate.[12]

In other cases, the character of the surface bond may depend on temperature or coverage. Piancastelli and co-workers studied adsorption of benzene on cleaved Si(111)-2×1 at low temperature and found that although chemisorption is energetically favorable at low coverage, physisorption becomes more favorable at a higher coverage.[13] With examples like this in mind, it becomes important to characterize adsystems that are approaching true physisorption, both from the perspective of ascertaining the physisorptive nature of the surface bond, and, if possible, to detect and describe departure from this limiting state. Inner-shell X-ray photoelectron spectroscopy (XPS) is recognized to be a useful tool for characterizing adsorbed species due to its strong surface sensitivity and, in principle, ease of interpretation. In line with the minimal-perturbation limit of physisorption, it is reasonable to expect large similarities between molecular spectra and spectra of physisorbed molecules on nonmetallic surfaces, as is often done.[1,6,7,14−18] However, little attention has been paid to how and why the spectra of such related yet disparate systems differ. To explore this point, a physisorbed condensate layer formed on top of a chemisorbed monolayer on silicon constitutes a close-to-ideal system.

To characterize organic adsorbate structures, carbon 1s (C1s) photoelectron spectra are acquired routinely. However, a typical C1s spectrum of an adsorbate system consists of one or a few broad peaks, with little structure to aid assignment. The source

* To whom correspondence should be addressed: E-mail: knut.borve@kj.uib.no.
[†] Department of Chemistry, University of Bergen.
[‡] Department of Physics and Technology, University of Bergen.
[§] Norwegian University of Science and Technology.

10.1021/jp1003352
Published on Web 08/23/2010

to additional line broadening in these spectra, compared to their molecular counterparts, is usually intrinsic to the adsorption system although often aggrevated by the use of X-rays with a substantial bandwidth. To understand the intrinsic, extra-molecular line broadening, it is useful to consider the adsorbent and the adsorbate layer together to constitute a polarizable environment for the adsorbing molecule. In the core-ionization event, extra-molecular relaxation takes place by polarizing this environment, stabilizing the spectroscopic final state through ion−dipole interaction. This mechanism opens for a distribution of core-ionization energies, corresponding to molecules in slightly different local surroundings and, in the multilayer case, also reflecting molecules in different layers. Intermolecular vibrations and phonon excitations associated with the ionization event as well as inelastic scattering of photoelectrons within the adsorbed layer may further affect spectra of adsorbed structures and contribute to line broadening and asymmetry in the lineshape.

Facing the typical low-structure carbon 1s spectrum of an adsorption layer, assigning the spectrum requires external information about which adspecies are present and what are their relative ionization energies. There are at least three different strategies to obtain this information. One is to apply computational chemistry; to optimize the structure of various possible adspecies and to compute relative ionization energies for these. However, such calculations are highly demanding and it is much more common to use calculations only to identify which are the more stable chemisorption structures.[1,19−21] Apart from narrowing down the field of adspecies to consider, spectral assigning is left to rely on one of the approaches considered next.

A second and powerful method for assigning is to compare a spectrum of an adsorbed structure (or "adsorption spectrum", for short) to a spectrum of an analogous system, if available. For example, it would be relevant to compare an adsorption spectrum to a spectrum of the same adsorbate on a related surface or in a related state.[7,14,18,20] Also, some authors make reference to gas-phase studies when assigning adsorption spectra.[6,16,17]

A third and common approach is to base assigning of peaks on *a priori* expectations of a certain ordering of ionization energies. One frequently made assumption is that, in the absence of electronegative or electropositive substituents, C1s ionization energies will group according to hybridization, with those of saturated (sp^3) carbons appearing at lower energy than those of unsaturated (sp^2 and sp) carbons.[1,2,5,18,20−22]

The purpose of the present work is 2-fold. Although it is reasonable to expect large similarities between spectra of gaseous and physisorbed molecules, the question of how a C1s photoelectron spectrum changes upon physisorption is by no means trivial. To further explore this, C1s spectra of 1,1-dichloroethene ($Cl_2C{=}CH_2$) and 1,3-cyclohexadiene were measured both for gaseous molecules and for molecules adsorbed on Si(111)-7×7. 1,1-Dichloroethene has a large internal shift in C1s ionization energy, and hence, any difference between a physisorption spectrum and a molecular spectrum is readily observed. 1,3-Cyclohexadiene is a typical example of an unsubstituted hydrocarbon adsorbate and has much smaller internal shifts.

Advances in experimental capabilities during the past two decades have made it possible to record gas-phase C1s photoelectron spectra with an instrumental broadening well below 0.1 eV, thereby providing access to vibrational fine structure as predicted by the Franck−Condon principle. There has been a corresponding development in theoretical methods, which allows for detailed modeling of the lineshape as well as relative ionization energies. By combining experimental and theoretical efforts one may, in many cases, provide an unambiguous interpretation of C1s spectra of quite complex medium-sized organic molecules.[23] The second purpose of this paper is to take advantage of the detailed assignments possible for molecular carbon 1s spectra to address the assumption made by many authors that, in general, sp^3 carbons have lower C1s ionization energies than do sp^2 hybridized carbons.[1,2,5,18,20−22] It is tacitly assumed that C1s ionization energies tend to cluster according to hybridization. More specifically, we challenge this commonly adopted rule-of-thumb in the specific cases of cyclopentene, propene and 1,3-cyclohexadiene and, more generally, by drawing on 46 accurately measured gas-phase ionization energies for 18 hydrocarbon compounds.

Experimental Procedures and Analysis

Soft X-ray photoelectron spectroscopy (XPS) studies of 1,1-dichloroethene (1,1-DCE) and 1,3-cyclohexadiene (1,3-CHD) adsorbed on the Si(111)-7×7 surface were performed using synchrotron radiation at beamline I311[24] at MAX-lab in Lund, Sweden. C1s spectra were recorded at normal emission using 330 eV photon energy. The experimental resolution was better than 0.09 eV. The surface was cleaned and checked as described in ref 25. Liquid 1,1-DCE (99%, Sigma-Aldrich) and 1,3-CHD (97%, Sigma-Aldrich) were cleaned by freeze−pump−thaw cycles.

Adsorption of 1,1-DCE and 1,3-CHD were performed by very similar procedures. First, chemisorption was carried out by stepwise exposing the Si(111)-7×7 surface to a total of 10 L sample at room temperature. The sample was cooled to 120 K and chemisorption spectra were measured. Next, the surface was exposed to another 10 L at 120 K, and a physisorbed layer formed on top of the chemisorbed molecules. The second set of C1s spectra contains contributions from both the chemisorbed and on-top physisorbed molecules. Because of low intensity close to the Fermi level, there exists no indigenous binding-energy reference for the adsorption spectra. The spectra are therefore plotted on a relative energy scale. The uncertainties of the relative ionization energies are estimated to 0.05 eV for 1,3-CHD and 0.03 eV for 1,1-DCE.

Gas-phase C1s photoelectron spectra of 1,1-DCE and cyclopentene were measured at beamline I411 at MAX-lab. Cyclopentene (Sigma-Aldrich, 98%) was measured at an instrumental resolution of 72 meV and a photon energy of 332 eV. For 1,1-DCE (99%, Sigma-Aldrich), the instrumental resolution was 70 meV and the photon energy 330 eV. Calibration of the ionization-energy scale was made with each compound mixed with CO_2, for which the ionization energy is well-known.[26] Based on experience from similar experiments,[26] the uncertainty of the absolute ionization energies is estimated to be 0.03 eV. The relative uncertainty is difficult to estimate, but may be as small as 0.01 eV. Because of the uncertainty in this quantity, three decimal places are retained for the gas-phase ionization energies.

The gas-phase spectra were fit using a set of theoretical, atom-specific lineshapes that take into account vibrational relaxation according to the Franck−Condon principle. For each site of ionization, the associated discrete Franck−Condon distribution is further convoluted with a lineshape function that accounts for lifetime broadening (100 meV[27]) and asymmetric distortion due to postcollision interactions (eq 12 in ref 28). Finally, it is convoluted with a Gaussian distribution to account for instru-

mental broadening, with a full width at half-maximum (fwhm) determined from analysis of the CO_2 peak in the calibration spectrum. The resulting lineshapes are used as motifs in a least-squares fit to the experimental spectrum, leaving the energy position and intensity of each lineshape and a constant background as the only free parameters. By routine, all permutations of the site-specific lineshapes are used as starting points in the fit. In many cases, the atom-specific lineshapes are sufficiently different to ensure that only one permutation gives a satisfactory fit of the experimental spectrum, as is the case for 1,1-DCE and 1,3-CHD. In other cases, exemplified by cyclopentene, an assumption of stoichiometric intensities is needed to achieve a meaningful result. By following this procedure, an unambiguous assigning of the spectrum is feasible and ionization energies can be determined with high accuracy (±0.03 eV).

In addition to the experimental data described above, this study also refers extensively to the gas-phase C1s photoelectron spectra of 1,3-CHD and propene, which were reported in refs 29 and 23, respectively. These data were obtained and analyzed with only very minor deviations from the procedures outlined above, and the resulting ionization energies are associated with the same uncertainty.

Computational Details

The calculation of Franck−Condon distributions requires access to optimized geometries, vibrational frequencies and normal mode vectors for both the ground state and each of the ionized states. For all compounds, vibrational frequencies and normal mode vectors were calculated using the hybrid density functional theory model B3LYP, in equilibrium structures obtained at the same level of theory. In the case of 1,1-DCE, the resulting Franck−Condon profiles did not match well with the recorded spectrum. This was resolved by recomputing the structural change that accompanies ionization using the highly accurate ab initio method CCSD(T), while retaining the normal-mode vectors and frequencies from the simpler theory. As for basis sets, carbon and hydrogen were represented using a Dunning triple-ζ basis[30] plus polarization functions[31] whereas chlorine was described using the triple-ζ basis set of McLean and Chandler[32] augmented with a double set of primitive polarization functions with d exponents α_d =1.50 and 0.375. For core-ionized carbon, the corresponding nitrogen basis was used with all exponents scaled by a factor of 0.9293.[33] To represent the core of the ionized carbon atom, the effective core potential by Stevens et al.[34] was scaled to account for only one electron in the 1s shell.[35] All calculations were carried out by means of the Gaussian 03 package of programs.[36]

The geometry of the dimer of 1,1-DCE was optimized using second order Møller−Plesset perturbation theory (MP2) in conjuction with cc-pVTZ basis sets for C and H and aug-cc-pVTZ for Cl[37,38] and with the counter-poise correction included at every step in the optimization.

A force-field was constructed to be used in rigid-body molecular dynamics calculations on a 55-molecular cluster of 1,1-DCE. Molecular geometries were obtained at the same level of theory as described above for the dimer and kept frozen in the molecular dynamics simulation. Functional forms and most force constants were taken from the AMOEBA force field[39,40] as implemented in the TINKER molecular modeling package version 5.1.[41] The full set of force-field parameters and molecular geometries is available as Supporting Information. The initial geometry of the 55-molecule cluster was prepared by positioning molecules with random orientation in an icosahedral array. Classical molecular dynamics was then run in the NVT ensemble with a time step of 1 fs at 90 K. After propagating the structure for half a nanosecond, equilibrium was reached as judged from kinetic and potential energies as well as structural parameters. The trajectory was then propagated another 0.5 ns and for the last 200 ps the structure was sampled every 1 ps and used for further analysis. For each of the 200 time frames, the shift in carbon 1s ionization energy relative to the molecular value is computed for each of the 2 × 55 sites of ionization in the cluster. The details of the procedure for computing shifts in inner-shell ionization energies by means of a polarizable force field are given in ref 42.

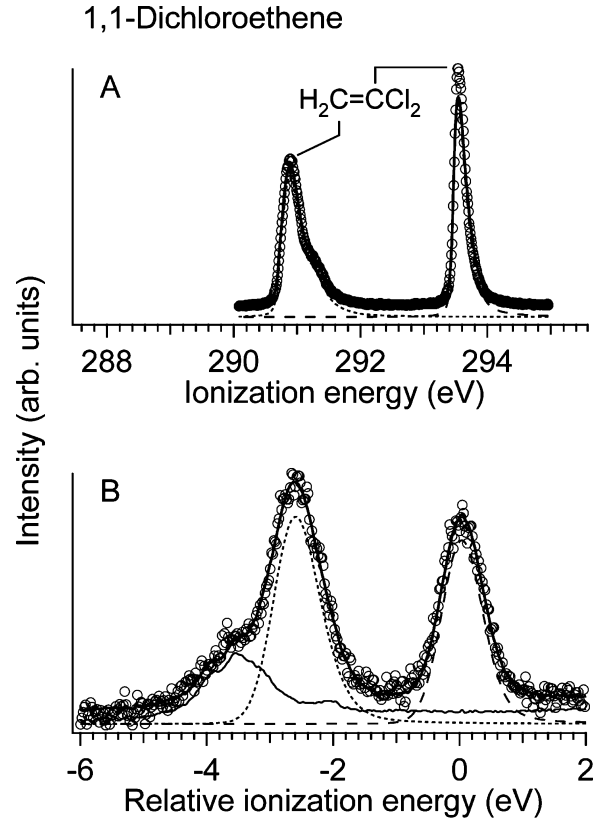

Figure 1. (A) C1s photoelectron spectrum of gaseous 1,1-DCE (circles). The overall fit (solid line) is the sum of two atom-specific theoretical lineshapes (dotted and dashed lines), one for each inequivalent carbon. (B) C1s photoelectron spectrum of 1,1-DCE adsorbed on a Si(111)-7×7 surface. The experimental spectrum (circles) contains contributions from both chemisorbed and physisorbed molecules. The overall fit (solid line) is a sum of theoretical lineshapes, one for each of the two carbons in the physisorbed layer (dotted and dashed lines), and the experimental C1s chemisorption spectrum (thin solid line). The vertical ionization energy for C1 in the physisorbed layer is chosen as zero-point for the energy axis.

Results

1,1-Dichloroethene. Figure 1 shows the C1s photoelectron spectra of 1,1-dichloroethene (1,1-DCE) in the gas phase (part A, top) as well as adsorbed on a Si(111)-7×7 surface (part B). The gas-phase spectrum displays two well-separated peaks corresponding to the inequivalent carbons in $CCl_2{=}CH_2$. The lineshapes are quite different for the two peaks and are in both cases closely reproduced by the theoretical atom-specific lineshapes (broken lines) constructed as described in a preceding section.

The most characteristic vibrational feature in a C1s spectrum is usually associated with symmetric C*−H stretching at the ionized carbon (C*), appearing at about 0.4 eV higher ionization

TABLE 1: Gas-Phase Adiabatic and Vertical Carbon 1s Ionization Energies for 1,1-Dichloroethene, 1,3-Cyclohexadiene, Cyclopentene, and Propene

			ionization energies (eV)	
molecule	carbon	hybridization	adiabatic	vertical
1,1-dichloroethene	C1	sp^2	293.516	293.577
	C2	sp^2	290.761	290.898
1,3-cyclohexadiene[a]	C1,C4	sp^2	289.912	290.07
	C2,C3	sp^2	290.124	290.28
	C5,C6	sp^3	290.497	290.69
cyclopentene	C1,C2	sp^2	289.988	290.137
	C3,C5	sp^3	290.372	290.553
	C4	sp^3	290.318	290.468
propene[b]	C1	sp^2	290.136	290.230
	C2	sp^2	290.612	290.759
	C3	sp^3	290.671	290.863

[a] Reference 29. [b] Reference 23.

energy if present.[43] The intensity ratio of the $\nu = 1$ to 0 peaks for this mode can be shown to be approximately proportional to the number of hydrogens bonded to C*,[44] which explains the significant difference between the C1 and C2 lineshapes for 1,1-DCE.

Only one of the two possible permutations of the theoretical lineshape models fits the experimental spectrum satisfactorily and allows for an unambiguous assigning of the low-energy peak to C2 (H_2C=). This conclusion is corroborated by the fact that chlorine has a much higher electronegativity than hydrogen, implying that carbon bonded to chlorine will have a higher 1s ionization energy than carbon bonded to hydrogen.

The use of theoretical lineshape models that include all important vibrational final states, allows us to identify the least energy required to ionize a given core orbital, i.e., the energy required to produce the corresponding ion in its vibrational ground state. This limiting ionization energy is known as the adiabatic energy, and for the present system we obtain adiabatic ionization energies of 290.761 eV for C2 (H_2C=) and 293.516 eV for C1 (=CCl_2). Moreover, access to the full Franck−Condon profile also allows us to calculate the average vibrational energy. Adding this to the adiabatic energy gives the vertical ionization energy, which represents the mean position of the peak. The resulting vertical ionization energies for 1,1-DCE are 293.577 eV for C1 and 290.898 eV for C2, which translates into a intramolecular chemical shift of 2.679 eV, see Table 1. The C1 peak has about 11% lower intensity than does C2, possibly due to different shakeup probabilities for the two carbons and scattering of the photoelectron on nearby chlorines.

In a second experiment, 1,1-DCE was first chemisorbed at room temperature on the Si(111)-7×7 surface and core-level photoelectron spectra recorded. A detailed analysis of the chemisorption process is presented in ref 25, which concluded that about one-third of the molecules break one carbon-chlorine bond while about two-thirds of them break both C−Cl bonds upon chemisorption. Three adspecies were observed on the surface, namely σ-bonded 1-chlorovinyl [(−CCl=CH_2), vinylidene (>C=CH_2, 1,1-bonded ethene) and silicon carbide.

Next, following the procedure outlined in the Experimental section, a physisorption overlayer of 1,1-DCE was deposited on top of the chemisorbed molecules. A second adsorption spectrum was then recorded which includes contributions from both chemisorbed molecules and the physisorbed overlayer, see Figure 1B. This spectrum was analyzed in terms of three contributions; one representing the chemisorbed molecules and one for each of the two carbon atoms in the physisorbed molecules. The first contribution was modeled by the experimental chemisorption spectrum, i.e., the spectrum recorded of the chemisorbed molecules before physisorption, see Figure 1B (thin solid line). To represent the physisorbed molecules, the atom-specific lineshapes introduced to fit the gas-phase spectrum in Figure 1A were included. However, as described in the Introduction, there are additional sources to line broadening in a physisorption spectrum compared to that of an isolated molecule. To account for this, the site-specific lineshape models were further convoluted by a Gaussian distribution with the respective fwhm left as free parameters in a fit to the experimental spectrum, together with the position and intensity of each component and a constant background.

From Figure 1B, it is evident that the combined chemisorption and physisorption spectrum of 1,1-DCE is very well fit by the described model. If the theoretical atom-specific lineshapes were to be interchanged, the value of the goodness-of-fit statistics χ^2 would increase significantly. Hence, even in the physisorbed state, the shape of the two peaks is sufficiently different to allow for unique assignment. The measured shift in vertical ionization energy between C1 and C2 in the physisorbed layer is 2.68 ± 0.03 eV, i.e., identical within error bars to the gas-phase shift. In sharp contrast to this apparent lack of sensitivity to the extramolecular environment, the optimized fwhm for the Gaussian distribution that represents the physisorption-related broadening is 0.70 eV for C1 and 0.66 eV for C2. Since the C1 peak is well separated from the chemisorption spectrum whereas the C2 peak partly overlaps with it, the first fwhm value of 0.70 eV is probably the more accurate of the two and will be at focus in the analysis. The total fwhm of the C1 peak is 0.85 ± 0.03 eV and the physisorption-related component is thus the dominating source to line broadening. An important point in the Discussion will be how such a large width can come about without affecting the intramolecular shift between C1 and C2.

There are three observations to report regarding the intensities. First, the intensity of the C1 peak drops to 79% of that of C2, and the deviation from stoichiometric proportions is thus larger than in the gas phase. Second, the chemisorption spectrum is still clearly discernible also after physisorption, cf. Figure 1. Judged from spectra for which the background has been normalized to the same value, the intensity of the chemisorption C1s spectrum drops by a factor of 0.7 ± 0.2 following the addition of the overlayer. Finally, the total peak area increases by a factor of 3.3 ± 0.5 based on the same C1s spectra, indicating that the physisorption layer contains at least twice as many carbon atoms as the chemisorbed layer.

In order to explore the propensity for molecular ordering of 1,1-DCE, and also to understand at a detailed level the increase in peak width from gas phase to the physisorbed phase, we undertook a computational study of the dimer as well as a fairly spherical cluster of 55 molecules.

The optimized dimer structure is one of a slipped, antiparallell arrangement of the two coplanar molecules, with a pointgroup symmetry of C_{2h} for the complex. Although the antiparallell arrangement provides a favorable dipole−dipole interaction, the molecules are displaced to a kite-like arrangement of the carbon atoms, bringing the chlorines closer and hence strengthening the van-der-Waals attraction. Hence, the shortest intermolecular carbon−carbon distance is between the two CCl_2 carbons, of 3.45 Å. The binding energy is computed to 13.5 kJ/mol.

Next, we turn to computational results for the 55-molecule cluster. Based on the radial mass density, the cluster has an inner, bulk-like part with fully coordinated molecules, and an outer, surface-like part with reduced number of nearest neigh-

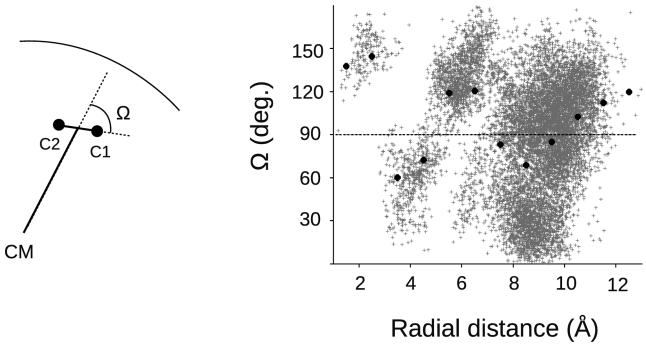

Figure 2. Molecular orientation in a cluster consisting of 55 molecules of 1,1-dichloroethene, described in terms of an angle Ω between the radial vector from the cluster center-of-mass (CM) to the midpoint of the C−C bond and the vector from C2 to C1 (left). To the right, Ω is given as a function of the radial distance R for all molecules as sampled during the production phase of the MD simulation. The mean value within bins of width 1 Å is added (filled circles).

bors. The mean distance from the cluster center-of-mass is 4.9 Å for the 11 molecules in the bulk fraction and 9.4 Å for the surface fraction which consists of 80% of the molecules. From Figure 2 there is a weak prevalence of surface molecules with the CCl_2 moiety directed inward as favored by van der Waal attractions.

For both of the inequivalent carbon atoms in 1,1-DCE, the 1s ionization energy is computed to be much lower in the $N = 55$ cluster than for the isolated molecule. This is as expected from other studies of molecular clusters and may be attributed to the presence of a polarizable extramolecular environment. More specifically, upon ionization, the surrounding molecules are polarized and the spectroscopic final state becomes stabilized by ion-dipole interactions, hence lowering the ionization energy. Considering molecules in different layers in the cluster, the reduction in ionization energy becomes more pronounced as one moves from the surface toward the center of the cluster, consistent with expectations based on the polarization model.

A second piece of information from the simulations, is that even within a single layer such as the surface, there is a significant spread in ionization energies. To be specific, the ionization energies of molecules in the surface layer are distributed fairly Gaussian, with a mean shift (ΔI) of −0.57 eV relative to that of the gas-phase molecule and with a fwhm of 0.37 eV. Looking into the importance of polarization effects (ΔP) vs contributions from permanent electrostatic moments at neighboring molecules (ΔM), one finds that the mean shift is almost exclusively due to polarization effects. However, the width of the distribution receives important contributions from both ΔM and ΔP. Looking at the individual distributions of M and P, the fwhm values are 0.37 and 0.20 eV, respectively. The large variation in the electrostatic component strengthens the notion that the molecules find themselves in different local surroundings. This leads to different electrostatic potentials at the sites of ionization, caused by the permanent and induced dipoles of neighboring molecules. From Table 2, it is evident that these considerations apply also to the bulk component, although with a numerically larger shift and somewhat narrower distributions. Clearly, there is a certain cancellation effect in that when the electrostatic potential is large, so is the counteracting polarization, making the ΔI distribution narrower than suggested by the widths of ΔM and ΔP.

1,3-Cyclohexadiene. Figure 3 shows the C1s photoelectron spectra of 1,3-CHD in the gas phase (part A, top) as well as adsorbed on a Si(111)-7×7 surface (part B). The molecular

TABLE 2: Computational Results for a 55-Molecule Cluster of 1,1-Dichloroethene

property	component	
	bulk	surface
number of molecules	11	44
mean distance[a] (Å)	4.90	9.41
ΔI, C1s shift relative to monomer (eV)	−0.76	−0.57
fwhm in C1s shift (eV)	0.31	0.37
contributions to ΔI:		
ΔP^b (eV)	−0.77	−0.56
ΔM^c (eV)	+0.01	−0.01
fwhm, ΔP^b (eV)	0.18	0.20
fwhm, ΔM^c (eV)	0.45	0.37

[a] From cluster center-of-mass. [b] Contribution to ΔI from polarization. [c] Contribution to ΔI from permanent electrostatic moments.

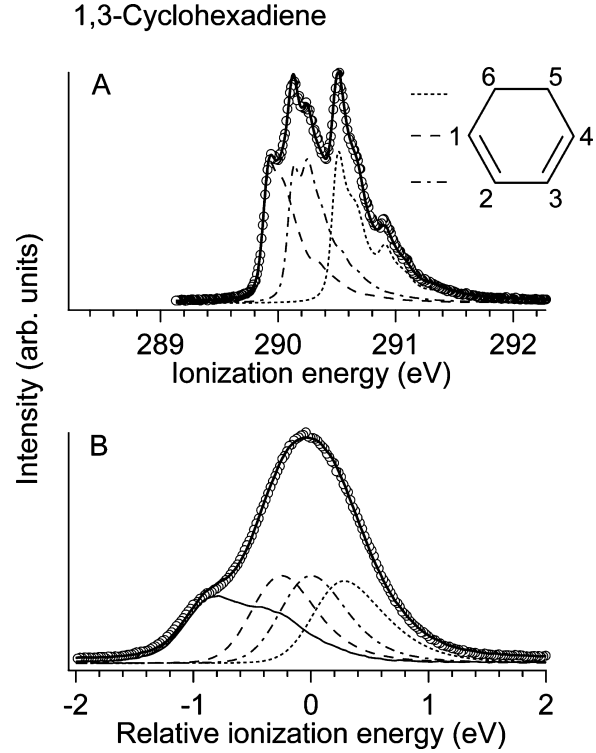

Figure 3. (A) C1s photoelectron spectrum of gaseous 1,3-CHD.[29] The total fit (solid line) of the experimental spectrum (circles) is a sum of three theoretical vibrational lineshapes (dotted and dashed lines). (B) C1s spectrum of 1,3-CHD physisorbed and chemisorbed to a Si(111)-7×7 surface. The experimental spectrum (circles) is fitted (solid line) by a least-squares procedure using four components. These are the experimental chemisorption spectrum (thin solid line) and the three theoretical lineshapes (broken lines) obtained from gas-phase modeling.

spectrum is published elsewhere[29] and is included here for comparative purposes. The spectrum was analyzed in ref 29 in terms of three atom-specific lineshape models corresponding to the three inequivalent carbons in this molecule; C1, C2, and C5. One of the six possible permutations stands out in terms of significantly lower χ^2 value in a fit to the experimental spectrum, thus providing an unambiguous assignment of the spectrum. This assignment is further corroborated by theoretical calculations of shifts in ionization energies.[29] The relative vertical ionization energies from this fit are given in Table 3. Of particular interest here is that the sp^2-hybridized carbons are found at lower ionization energy than the sp^3 carbon (C5). The difference in ionization energy between the two inequivalent sp^2 carbons is significant and about half of the smallest sp^3-sp^2 (C5−C2) shift in this molecule, cf Table 1.

TABLE 3: Relative Vertical[a] Ionization Energies (eV)

carbon	hybridization	gas phase[b]	physisorbed
1,4	sp^2	−0.22	−0.24
2,3	sp^2	0.00	0.00
5,6	sp^3	0.39	0.32

[a] In both cases, the energy of the C2,C3 peak is used as internal reference. [b] From ref 29.

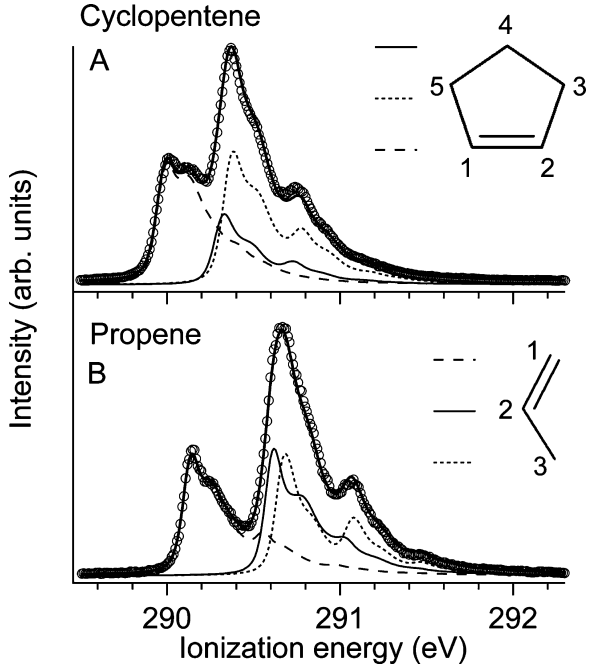

Figure 4. C1s photoelectron spectrum (circles) of gaseous cyclopentene (A) and propene (B). Fits of the spectra are prepared as sums (solid line) of three theoretical, vibrational lineshapes, one for each inequivalent carbon atom (broken lines).

Turning to the C1s spectrum of 1,3-CHD adsorbed on a Si(111)-7×7 surface, see Figure 3B, one finds that the spectrum contains contributions from both chemisorbed molecules and an on-top physisorbed layer. The procedure described for 1,1-DCE was applied when fitting this spectrum, except that the intensities and the Gaussian widths of the three theoretical lineshapes were constrained to be equal. While the vibrational structure was important when assigning the gas-phase spectrum, lack of structure in the adsorption spectrum of 1,3-CHD allows any permutation of the atom-specific lineshapes to be used without significant change in the quality of the fit. We have therefore made recourse to the energy ordering from the gas-phase measurements where it was defined unambiguously. Compared to the relative ionization energies measured in the gas phase, the shift in ionization energy between the two types of sp^2-hybridized carbons is not significantly changed for the physisorbed state while the shift between the peaks corresponding to C2/C3 and C5/C6 is slightly reduced, see Table 3. The extra Gaussian broadening of the spectrum associated with the physisorption state is given by a fwhm of 0.47 eV. This is significantly lower than what was observed for 1,1-DCE (0.70 eV).

Gaseous Cyclopentene and Propene. The C1s photoelectron spectrum of gaseous cyclopentene is shown in Figure 4A. The molecule has C_s symmetry, making the sp^2 carbons (C1 and C2) equivalent and also C3 and C5. The spectrum was fitted following the procedure already described. In this case, the sp^3 hybridized carbons (C3/C5 and C4) are all bonded to two hydrogen atoms and hence the atom-specific lineshapes turn out very similar. In order to obtain a well-defined model, a constraint on the relative intensity of C5/C3 to C4 to be stoichiometric, i.e., equal to 2:1, was imposed. The agreement between the fit and the experimental spectrum leaves no doubt about the assignment, cf. Figure 4, and the resulting ionization energies are summarized in Table 1. The sp^2 carbons have an experimental adiabatic ionization energy of 289.988 eV, which is significantly below the corresponding values for the sp^3-hybridized carbons: 290.372 eV for C3/C5 and 290.318 eV for C4. The small shift between the sp^3 carbons and the similarity of the corresponding lineshapes, implies that in this specific case, the spectrum could have been fit using a single lineshape model common to the sp^3 carbons.

Whereas cyclopentene contains two inequivalent sp^3 carbons and one unique sp^2 carbon, propene has two inequivalent sp^2 carbons and a single sp^3 carbon. The gas-phase carbon 1s photoelectron spectrum of propene was published in ref 23 and analyzed using the same procedure as described in the present work. The spectrum is included in Figure 4B together with atom-specific lineshape models. The vibrational structure leaves no doubt about the assignment, and the resulting ionization energies are included in Table 1. As for cyclopentene, the lowest 1s ionization energy is found for one of the sp^2 carbons, namely the terminal one (C1). Noteworthy, the other sp^2 carbon has an ionization energy that is almost 0.5 eV higher, which takes it close to that of the methyl carbon.

Discussion

Comparison of Gas-Phase Spectra and Spectra of Adsorbed States. For 1,1-dichloroethene (1,1-DCE), we find that a broadened gas-phase spectrum serves as a good model for the carbon 1s photoelectron spectrum of the physisorbed species. The intramolecular shift between C1 and C2 is identical within error bars for the two states, at 2.68 ± 0.03 eV. McFeely and co-workers made a similar observation for the related system chloroethane physisorbed on hydrogenated Si(111).[45] They were primarily interested in whether proximity to a polarizable surface would affect shifts associated with intramolecular second-nearest-neighbor interactions and found the splitting between the two peaks in chloroethane to be 1.15 ± 0.1 eV in the physisorbed state to be compared to a vertical gas-phase shift of 1.17 ± 0.10 eV.[46] For 1,3-cyclohexadiene (1,3-CHD) there is some evidence for a small increase in the shift between the sp^3 carbons on the one hand, and the sp^2 carbons on the other. A possible explanation may be closer intermolecular packing of the flat end of the molecule, thus enhancing the intermolecular electronic relaxation.

Returning to 1,1-DCE, the C1-to-C2 intensity ratio is seen to drop from 0.89 in the gas phase to 0.79 in the physisorption state. In the molecular case, it was suggested that the departure from stoichiometric intensities may possibly be due to different shakeup probabilities for the two carbons and scattering of the photoelectron on nearby chlorines. Both of these explanations involve the virtual orbital space, which is known to be less localized and quite sensitive to the intermolecular surrounding. From this perspective, a change in the intensity ratio from gas phase to the physisorption state is not unreasonable. The alternative explanation of a change in C1-to-C2 intensity ratio due to orientational effects seems less likely. Molecular dynamics simulations gave only a slight tendency for the surface molecules of the 55-cluster to co-orient the methylene ends out of the cluster, cf. Figure 2. This result is corroborated by our finding that the most stable structure of the dimer is one of displaced, antiparallell monomers, consistent with a favorable dipole−dipole interaction. Both of these results suggest that at least the top physisorbed layer does not contain a strong dominance of either C1 or C2 at the outer surface at the temperature considered here (120 K).

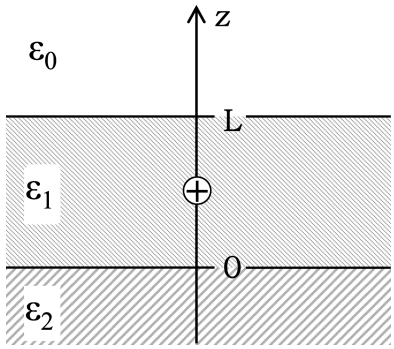

Figure 5. Dielectric continuum model for polarization effects on the dependency of the shift in core-level ionization energy on the vertical position in the adlayer.

An important issue in adsorption studies is the depth of the adlayer which in principle may be addressed by considering how the photoelectron current changes with surface preparation. Quantitative analysis of XPS intensities is usually based on an exponential *Ansatz* for the attenuation of the photoelectron signal due to interaction with matter over a distance z, as

$$I/I_0 = \exp(-z/\lambda) \quad (1)$$

The attenuation length, λ, depends on both the kinetic energy of the photoelectron and the medium through which the electrons propagate, and it is closely related to the mean-free-path between inelastic scattering events. Equation 1 may be applied to the C1s signal from the chemisorbed layer of 1,1-DCE, assuming that the physisorbed layer has a thickness of d. Since the intensity of this signal was found to drop by a factor of 0.7 ± 0.2 following the addition of the overlayer, and this implies that $d/\lambda = -\ln 0.7 = 0.4 \pm 0.3$. Moreover, applying the integrated form of eq 1 to the observed relative increase in total peak area following physisorption, given as 3.3 ± 0.5 and combining it with $\exp(-d/\lambda) = 0.7$, one obtains a thickness of the chemisorption layer of about one-third of the physisorption layer. Since the chemisorbed layer is limited to a monolayer, this lets us arrive at an estimate of three molecular layers in the physisorbed overlayer.

The most striking change in the carbon 1s spectrum of 1,1-DCE upon physisorption is the increased line width, in the case of C1 amounting to convolution of the gas-phase spectrum of a Gaussian with fwhm of 0.70 eV. The cluster simulation provides useful estimates of the distribution of ionization energies within a cluster shell, summarized by a fwhm value of 0.37 eV for the surface layer and 0.31 eV for the 11-molecule bulk part. Although these numbers are certainly affected by the curvature of the surface, they probably still give resonable estimates of the layer-intrinsic part of the width. An additional contribution to the observed width in the physisorption spectrum comes from the change in mean ionization energy as one progresses from the topmost layer toward the silicon adsorbent, modulated by attenuation of the photoelectron current. A first estimate may again be obtained from the cluster simulations, which gave a shift of 0.19 eV between the surface and bulk components. The preceding paragraph suggests that it is of interest to consider a somewhat thicker adsorption layer and also to take into account the nature of the adsorbent, and to this end, we introduce a continuum model of the adsorption system.

In the continuum model, both adsorbent and the adsorbed phase are considered to be flat and structureless dielectric substrates. The geometry as shown in Figure 5 consists of three regions that are stacked in the z direction and infinitely wide in directions perpendicular to z. Region II is a linear dielectric substrate of optical permittivity of ε_2 extending from $z = 0$ and infinitely far in the negative z direction, representing the solid adsorbent. Region I represents a condensation layer of thickness L; it has an optical permittivity of ε_1 and extends from $z = 0$ to L. Above the film, i.e., at $z > L$, there is vacuum and hence permittivity, ε_0.

We are concerned with how the polarization energy varies with the depth at which a core ion is created within an adlayer of given thickness L. In the Appendix, we present a simple derivation of such an expression, eq 8, by solving Poisson's equation for the electrostatic problem defined by our model. To apply it to the present system, we use the refractive index and the density of liquid 1,1-DCE[47] to estimate respectively the (optical) dielectric constant to 2 and the thickness of a single close-packed layer of 1,1-DCE to 5 Å. Similarly, a dielectric constant of 15 is used for silicon.[48] With an assumption of a total of four molecular layers on top of silicon, one of which is a model of the chemisorbed monolayer, we obtain a shift of 0.19 eV in core-level ionization energy between layer 1 and 2 counting from the vacuum side, in very good agreement with the cluster result. The shift between layer 2 and 3 is smaller: 0.10 eV. Using these energies in conjunction with the photoelectron attenuation model (eq 1) and the theoretical lineshape model for the C1 peak in 1,1-DCE, gives a total line width (fwhm) for layers 1−3, i.e., the physisorption part, of just below 0.5 eV for λ between 10 and 20 Å. For comparison, the theoretical lineshape model for C1 has a fwhm of about 0.19 eV.

Combining the line broadening computed within a single surface layer for the cluster (0.37 eV, cf Table 2) with the total line width obtained for the continuum model, gives a fwhm of 0.6 eV. This number still undershoots the observed width in the adsorption spectrum of 1,1-DCE, but taking into account the simplicity of the continuum model, the agreement is satisfactory. One missing factor is intermolecular vibrational relaxation associated with the ionization event. In clusters of methanol, the corresponding fwhm was computed to 0.27 eV.[42] On account of the weaker intermolecular forces in the present system, we consider this an upper limit for 1,1-DCE.

We now turn attention to the carbon 1s spectrum of 1,3-CHD, where the vibrational lineshapes are more similar to one another and the internal shifts are smaller. Even though the physisorption spectrum presented here was acquired using high-resolution synchrotron radiation, a unique assignment of the spectrum is not possible based solely on the experimental data. Obviously, the ability to draw firm conclusions about assignment is usually even more limited for C1s spectra acquired using conventional X-ray sources. Thus, one has to rely on information external to the spectrum in order to arrive at a unique assignment. We suggest that if gas-phase C1s ionization energies are available, these may provide a viable starting point for the analysis of physisorption spectra. A molecule retains its covalent bonds when physisorbing and, hence, has the same possibilities for intramolecular charge distribution and redistribution as in the gaseous state. Extramolecular polarization can give minor changes in internal shifts. However, only in cases when the internal shift is too small to be resolved would one expect the extramolecular polarization to change the relative positions of the peaks. An interesting exception is found for n-octane on Cu(100), for which the carbon 1s photoelectron spectrum of the monolayer is actually narrower than the molecular spectrum.[49] This may be taken as indicative of a surface bond that challenges the classification as physisorption.[12]

Whereas the physisorption-related spectral broadening for 1,1-DCE amounts to fwhm values of 0.70 and 0.66 eV for C1 and C2, respectively, the corresponding fwhm was determined to 0.47 eV in the case of 1,3-CHD. The continuum model introduced above suggests that line broadening due to multilayer formation should be quite similar between the two systems. The cluster model may shed some light on this issue. From the simulations for 1,1-DCE, we saw that the dispersion of core ionization energies within a layer was largely due to the permanent electrostatic moments. In the gas phase, the permanent dipole moment of 1,3-CHD is only one-third of that of 1,1-DCE. In the condensed phase, the latter is likely to increase further. Hence, one contribution toward less physisorption-induced broadening in the case of 1,3-CHD compared to 1,1-DCE, may be a more homogeneous electrostatic potential within each adsorption layer.

What Is the Relationship between C1s Ionization Energies and Hybridization? As pointed out in the Introduction, many authors base their assignment of C1s spectra on the assumption that C1s ionization energies group according to hybridization, with those of saturated (sp^3) carbons appearing at lower energy than those of unsaturated (sp^2, sp) carbons. Examples include molecules like cyclopentene,[2,18,20] cyclohexene,[21] 1,3-CHD,[21] 1,4-cyclohexadiene,[18,21] 1,5-cyclooctadiene,[1] acetylethyne,[5] and 3-pyrroline.[2] According to ref 2, the assumption seems in part to have been motivated by early gas-phase measurements of the three C_2 molecules displaying each of the hybridization states mentioned above, namely ethane (H_3C-CH_3; sp^3), ethene ($H_2C=CH_2$; sp^2), and ethyne ($HC\equiv CH$; sp). For these molecules the C1s ionization energy does indeed increase with carbon−carbon bond order.[50] However, it is not obvious that the energy ordering obtained for these simple molecules, containing only one kind of carbon atoms, carries over to molecules which contains both saturated and unsaturated carbons. This point will be examined by means of data for gaseous cyclopentene, propene and 1,3-CHD as well as gas-phase ionization energies for another 15 saturated and unsaturated hydrocarbons.

From the analysis of cyclopentene, we see that the two inequivalent sp^3 carbons differ only slightly in their ionization energies, effectively allowing the C1s ionization energies to group according to hybridization. However, the energy ordering is the opposite of what many authors assume: the highest ionization energy is found for the sp^3-hybridized carbon atoms, not the sp^2-hybridized ones. Turning to 1,3-CHD, the two inequivalent sp^2 carbons have significantly different ionization energy, and again the highest ionization energy is found for the sp^3-hybridized carbon atoms.

The C1s spectrum of propene shows two pronounced peaks with intensity ratio close to 1:2 and with the low-energy peak carrying the least intensity, cf. Figure 4. This appears to fit well with an *a priori* assumption of ionization energies based on hybridization; assigning the low-energy, low-intensity peak to the methyl carbon and the two sp^2 carbons to the strong peak at 0.5 eV higher ionization energy. From the Results section, it is clear that such an assignment is wrong for two out of the three carbon atoms in this molecule and hence imply a complete misinterpretation of the spectrum.

1,3-CHD, and propene exemplify that carbons that share hybridization state in the same molecule can have both similar and dissimilar ionization energies and that assuming carbons of the same hybridization to have similar ionization energies may give very wrong results. Furthermore, the assumption that unsaturated carbon atoms have higher ionization energies than saturated ones, does not apply for any of these molecules.

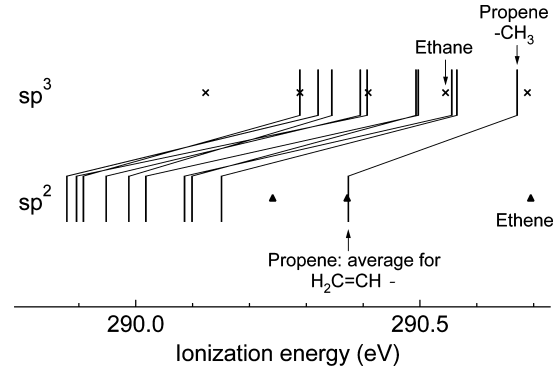

Figure 6. Adiabatic carbon 1s ionization energies grouped according to the hybridization of the ionized atom. The bars represent average sp^3 and average sp^2 ionization energies for ten compounds containing carbons of both hybridizations. For each of these compounds, the two average ionization energies are connected with lines. The crosses and triangles represent average ionization energies for compounds where all carbons have the same hybridization.

To further illustrate this point, Figure 6 shows how the adiabatic ionization energies of 18 pure hydrocarbons group according to the hybridization of the ionized atom. For compounds having several inequivalent carbons with the same hybridization, the average ionization energy for each hybridization is plotted. A full overview of all the ionization energies is given in ref 51. Ten compounds having both sp^2 and sp^3 hybridized carbons are included. Taking propene as an example, the ionization energy of the sp^3 carbon is plotted in the upper part of the figure, while the average ionization energy for the two sp^2 carbons is plotted in the lower part. The two bars representing each of these ionization energies are connected with a line. Data for 1,3-CHD, cyclopentene, 1,3-pentadiene,[23] *trans*-3-hexene, cyclohexene,[29] 1,4-cyclohexadiene,[29] methylbenzene (toluene),[52] 1,3-dimethylbenzene (*m*-xylene),[52] and 1,4-dimethylbenzene (*p*-xylene)[52] are plotted in the same way. The five compounds represented by crosses in Figure 6 have only sp^3 carbons and include methane,[26] ethane,[26] propane,[33] butane,[33] and cyclohexane.[29] Ethene,[26] 1,3-butadiene,[23] and benzene[53] have only sp^2 carbons and are represented by triangles.

For each hybridization state, we see that the ionization energies are distributed over a fairly wide energy range (0.6−0.8 eV) and these energy ranges are largely overlapping between sp^3 and sp^2. As mentioned, the ionization energies of ethane and ethene have been used as general examples to indicate the order of ionization energies of sp^3 and sp^2 carbons.[2] From the figure, we see that the sp^3 carbons of ethane have a lower ionization energy than the sp^2 carbons of ethene. However, in molecules having both saturated and unsaturated bonds, the average sp^2 ionization energy is lower than the average sp^3 ionization energy, i.e., quite opposite to the assumption made for instance in refs 1, 2, 5, 18, and 20−22. The reason for this can be found in the ability that these molecules have to delocalize charge upon ionization. A saturated (i.e., sp^3-hybridized) carbon atom in neighboring (α) position to a carbon−carbon π bond, like in C_α-C=C, tends to donate electrons to the farthest carbon atom in the π bond, to give a charge distribution $C_\alpha(+\delta)$-C=C$(-\delta)$ and corresponding shifts in C1s ionization energies.[23,54,55] Within organic chemistry, this finding is often explained in terms of valence-bond theory as hyperconjugation; see ref 56 for details. Evidently, the choice of ethane and ethene as model compounds is unjustified.

In Figure 6, there is a clear tendency of the average sp^2 ionization energy in a molecule to be lower than the corresponding sp^3 value,

and it is reasonable to ask if this can be used in assigning physisorption spectra. Our answer is, however, negative. Although the average energies show a systematic behavior, this trend does not carry over to the individual ionization energies. Six of the eighteen molecules have more than one inequivalent sp^2 carbon. Among these six, the intramolecular shift in sp^2 ionization energies ranges from 0.21 eV in 1,3-CHD to 0.74 eV in 1,3-pentadiene. Thus, the span in sp^2 energies is of the same order as the difference between average sp^3 and sp^2 ionization energies and any *a priori* assumption of ionization energies based on hybridization may easily lead to misinterpretation of spectra, as shown in the example of propene.

Concluding Remarks

For 1,1-dichloroethene physisorbed on Si(111)-7×7, the gas-phase spectrum provides an excellent model of the C1s photoelectron spectrum of the physisorbed state, both with respect to peak shapes and internal shifts in ionization energies. A similar comparison for 1,3-cyclohexadiene reveals only small changes in relative ionization energies between the gaseous and the physisorbed state. These two systems demonstrate that the main difference in carbon 1s spectra recorded for the same molecule in the gas phase and in a physisorbed state is additional broadening due to a distribution of ionization energies within each molecular layer as well as across a multilayer condensate. We suggest that assignment of photoelectron spectra of physisorbed molecules be based on gas-phase spectra of the same compounds, and that simple models may be useful to gain insight in the line-broadening mechanims in these systems. This facilitates the construction of model spectra prior to experiments, which may be helpful in identifying systems on the borderline between physisorption and chemisorption.

An important aim of this work was to explore the validity of an assumption often invoked when assigning C1s photoelectron spectra of adsorbed molecules, namely that the ionization energies group according to hybridization and, moreover, that unsaturated carbon atoms have higher ionization energies than do saturated carbons.[2] In cyclopentene, the C1s energies do in fact group according to hybridization, while the opposite is found to be the case for propene and with 1,3-cyclohexadiene as a border case. In all three molecules, the highest ionization energy is actually found for sp^3-hybridized carbons, rather than the unsaturated ones. Hence, we advice against assigning carbon 1s spectra based on hybridization, as this may easily lead to misinterpretation as clearly demonstrated in the example of propene. Rather, an unambiguously assigned gas-phase spectrum of the adsorbate may constitute a highly useful reference in many physisorption studies.

Acknowledgment. We are pleased to thank Ingeborg-Helene Svenum and the MAX-lab staff for their assistance during the beamtime. This work was supported by the Research Council of Norway (NANOMAT programme, Contract No. 158516/S10 for T.H.A.), the Nordic Research Board (NORDFORSK), and the Norwegian High Performance Computing Consortium NOTUR. Economical support was also received from the European Community−Research Infrastructure Action under the FP6 "Structuring the European Research Area" Programme (through the Integrated Infrastructure Initiative "Integrating Activity on Synchrotron and Free Electron Laser Science").

Appendix

We consider a schematic model defined by three regions that are stacked in the z direction and infinitely wide in the directions perpendicular to z. Region II is a linear dielectric substrate of optical permittivity of ε_2 extending from $z = 0$ and infinitely far in the negative z direction, representing the solid adsorbent. Region I represents a condensation layer of thickness L; it has an optical permittivity of ε_1 and extends from $z = 0$ to L. Above the film, i.e., at $z > L$, there is vacuum and hence permittivity ε_0. The polarization energy associated with the sudden creation of a charge e at position $\zeta\mathbf{e}_z$ in the condensation layer ($\mathbf{e}_z$ is a unit vector on the z axis) is most conveniently found in terms of the electric potential ϕ, which is found by solving Poisson's equation $\nabla^2\phi = -(q/\varepsilon)\delta(\mathbf{r} - \zeta\mathbf{e}_z)$. The unique solution to this equation is sought as the sum of two parts of which the first is a particular solution to Poisson's equation that takes into account the explicit charge in the condensation layer albeit without observing boundary conditions. The second component starts out from the general solution to the homogeneous (Laplace) equation, $\nabla^2\phi = 0$, but made specific by requiring that the final solution should obey continuity conditions at the boundaries.

In the middle region and without regard for boundary conditions, a particular solution to Poisson's equation is obtained as

$$\phi_P(r,z) = \frac{q}{4\pi\varepsilon_1}\frac{1}{\sqrt{r^2 + |z-\zeta|^2}} = \frac{q}{4\pi\varepsilon_1}\int_0^{+\infty} e^{-k|z-\zeta|}J_0(kr)\,dk \quad (2)$$

A complete set of solutions to Laplace's equation in sylindrical coordinates may be found by the factorization method, see for instance ref 57. Requiring the solutions to be independent of the azimuthal angle, regular for large values of the distance r to the z axis and also regular at the z axis, leads to the following expression:

$$\phi_L(r,z) = \frac{q}{4\pi\varepsilon}\int_0^{+\infty}[A(k)e^{-kz} + B(k)e^{kz}]J_0(kr)\,dk \quad (3)$$

In region II, $A(k) = 0$ in order to keep the potential finite, and for the same reason, $B(k) = 0$ in the vacuum region. Hence, the relevant expression for the homogeneous solution becomes

$$\phi_L(r,z) = \frac{q}{4\pi}\begin{cases}\frac{1}{\varepsilon_0}\int_0^{\infty} A_0(k)e^{-kz}J_0(kr)\,dk & z > L\\ \frac{1}{\varepsilon_1}\int_0^{\infty}(A(k)e^{-kz} + B(k)e^{kz})J_0(kr)\,dk & 0 < z < L\\ \frac{1}{\varepsilon_2}\int_0^{\infty} B_2(k)e^{kz}J_0(kr)\,dk & z < 0\end{cases}$$

The boundary conditions are that the potential $\phi = \phi_P + \phi_L$ as well as the electric displacement normal to the boundary, $-\varepsilon(\partial\phi/\partial z)$, should be continuous on the boundaries. These two conditions applied at the boundaries $z = 0$ and L provide the four equations necessary to determine A_0, A, B, and B_2. In terms of $\Delta_r = (\varepsilon_1 - \varepsilon_r)/(\varepsilon_1 + \varepsilon_r)$, $r = 0,\ 2$, and $x = \Delta_0\Delta_2$, we obtain

$$B(k) = \frac{e^{-2kL}}{1 - xe^{-2kL}}(\Delta_0 e^{k\zeta} + xe^{-k\zeta}) \quad (4)$$

and

$$A(k) = \Delta_2 e^{-k\zeta} + \Delta_2 B(k) \quad (5)$$

Apart from the self-energy of the point charge, the electrostatic energy of the system is given by $U = {}^1/_2 q\phi'(\zeta \mathbf{e}_z)$, where the prime indicates exclusion of the term divergent at the position of the point charge. Hence

$$U = \frac{q^2}{8\pi\varepsilon_1}\int_0^\infty A\mathrm{e}^{-k\zeta} + B\mathrm{e}^{k\zeta}\,\mathrm{d}k \tag{6}$$

since $J_0(0) = 1$. Inserting eqs 4 and 5 into eq 6, one obtains

$$U = \frac{q^2}{8\pi\varepsilon_1}\int_0^\infty \Delta_2\mathrm{e}^{-2k\zeta} + \frac{\mathrm{e}^{-2kL}}{1 - x\mathrm{e}^{-2kL}}(\Delta_0\mathrm{e}^{2k\zeta} + 2x + x\Delta_2\mathrm{e}^{-2k\zeta})\,\mathrm{d}k \tag{7}$$

By drawing on formula 3.311.4 in ref 58, introducing $s = \zeta/L$ and combining the resulting terms, one obtains

$$U = \frac{q^2}{4\pi\varepsilon_1 L}\left(\frac{1}{4}\Delta_0\sum_{i=0}^{\infty}\frac{x^i}{i+1-s} + \frac{1}{4}\Delta_2\sum_{i=0}^{\infty}\frac{x^i}{i+s} - \frac{1}{2}\ln(1-x)\right) \tag{8}$$

Essentially the same expression is given as eq A18 in ref 59, obtained in a different context and by using the image-charge technique. The $i = 0$ terms in the two sums are singular at the boundaries. In ref 59, this is remedied by introducing a phenomenological "mirror shift", i.e. adding a positive damping constant in the denominator of the two singular terms. A similar situation arises if we consider a planar interface between only two dielectrics, i.e., by setting $\varepsilon_0 = \varepsilon_1$, in which case the polarization energy becomes $U = (q^2/4\pi)(\Delta_2/4\varepsilon_1\zeta)$. Again a singularity is apparent at the boundary, and in refs 60 and 61, it is proposed to apply this expression only outside a distance h of the interface and then assume the polarization energy to be constant closer to the interface. The appropriate value for h is determined by reference to the Born energy of solvation and found to be equal to half the Born radius of the solvated ion. We obtain the same value for h when applying this approach to the present system. A more advanced approach is advocated in ref 62 in which the ionized atom or molecule is embedded in a cluster of induced point dipoles that are determined in a self-consistent manner, and leaving only the polarization contribution from the far-away dipoles to be included in the continuum limit.

Returning to eq 8 to describe a shift in ionization energy within the condensation layer, one recognizes that the last term is relevant only when comparing films of different thickness as it is independent of position within the adsorbate layer. The two first terms in eq 8 provide the chemical shift due to polarization of neighboring molecules and the adsorbent between molecules at different depth in the condensate layer.

Supporting Information Available: Full set of force-field parameters and molecular geometries for rigid-body molecular dynamics simulations of 1,1-dichloroethene. This material is available free of charge via the Internet at http://pubs.acs.org.

References and Notes

(1) Hovis, J. S.; Hamers, R. J. *J. Phys. Chem. B* **1997**, *101*, 9581–9585.

(2) Liu, H.; Hamers, R. J. *Surf. Sci.* **1998**, *416*, 354–362.

(3) Jolly, F.; Bournel, F.; Rochet, F.; Dufour, G.; Sirotti, F.; Taleb, A. *Phys. Rev. B* **1999**, *60*, 2930–2940.

(4) Kong, M. J.; Teplyakov, A. V.; Jagmohan, J.; Lyubovitsky, J. G.; Mui, C.; Bent, S. F. *J. Phys. Chem. B* **2000**, *104*, 3000–3007.

(5) Huang, H. G.; Cai, Y. H.; Huang, J. Y.; Tang, H. H.; Xu, G. Q. *Langmuir* **2005**, *21*, 3384–3388.

(6) Gunnella, R.; Shimomura, M.; D'Amico, F.; Abukawa, T.; Kono, S. *Phys. Rev. B* **2006**, *73*, 235435−1–7.

(7) Letarte, S.; Adnot, A.; Roy, D. *Surf. Sci.* **2000**, *448*, 212–218.

(8) Tao, F.; Qiao, M. H.; Li, Z. H.; Yang, L.; Dai, Y. J.; Huang, H. G.; Xu, G. Q. *Phys. Rev. B* **2003**, *67*, 115334−1-7.

(9) Tao, F.; Qiao, M. H.; Wang, Z. H.; Xu, G. Q. *J. Phys. Chem. B* **2003**, *107*, 6384–6390.

(10) *Manual of symbols and terminology for physiochemical quantities and units*; Everett, D. H., Ed.; Butterworths: London, 1970; Appendix II, Part I, p 586.

(11) Adamson, A. W. *Physical Chemistry of Surfaces*, 5th ed.; John Wiley & Sons, Inc.: New York, 1990; p 382.

(12) Öström, H.; Triguero, L.; Nyberg, M.; Ogasawara, H.; Pettersson, L. G. M.; Nilsson, A. *Phys. Rev. Lett.* **2003**, *91*, 046102-1−046102-4.

(13) Piancastelli, M. N.; Kelly, M. K.; Chang, Y.; McKinley, J. T.; Margaritondo, G. *Phys. Rev. B* **1987**, *35*, 9218–9221.

(14) Fink, A.; Widdra, W.; Wurth, W.; Keller, C.; Stichler, M.; Achleitner, A.; Comelli, G.; Lizzit, S.; Baraldi, A.; Menzel, D. *Phys. Rev. B* **2001**, *64*, 045308−1-9.

(15) Yamashita, Y.; Machida, S.; Nagao, M.; Yamamoto, S.; Mukai, K.; Yoshinobu, J. *Chem. Phys. Lett.* **2003**, *374*, 476–481.

(16) Papp, C.; Denecke, R.; Steinrück, H.-P. *Langmuir* **2007**, *23*, 5541–5547.

(17) D'Amico, F.; Gunnella, R.; Shimomura, M.; Abukawa, T.; Kono, S. *Phys. Rev. B* **2007**, *76*, 165315−1-8.

(18) Passmann, R.; Bruhn, T.; Nilsen, T. A.; Fimland, B. O.; Kneissl, M.; Esser, N.; Vogt, P. *Phys. Status Solidi B* **2009**, *246*, 1504–1509.

(19) Ellison, M. D.; Hovis, J. S.; Liu, H.; Hamers, R. J. *J. Phys. Chem. B* **1998**, *102*, 8510–8518.

(20) Lee, S. W.; Hovis, J. S.; Coulter, S. K.; Hamers, R. J.; Greenlief, C. M. *Surf. Sci.* **2000**, *462*, 6–18.

(21) Tao, F.; Wang, Z. H.; Xu, G. Q. *Surf. Sci.* **2003**, *530*, 203–215.

(22) Passmann, R.; Favero, P.; Schmidt, W. G.; Miotto, R.; Braun, W.; Richter, W.; Kneissl, M.; Esser, N.; Vogt, P. *Phys. Rev. B* **2009**, *80*, 125303−1-7.

(23) Thomas, T. D.; Sæthre, L. J.; Børve, K. J.; Gundersen, M.; Kukk, E. *J. Phys. Chem. A* **2005**, *109*, 5085–5092.

(24) Nyholm, R.; Andersen, J. N.; Johansson, U.; Jensen, B. N.; Lindau, I. *Nucl. Instr. Meth. Phys. Res. A* **2001**, *467−468*, 520–524.

(25) Andersen, T. H.; Zahl, M. G.; Svenum, I. H.; Børve, K. J.; Borg, A.; Sæthre, L. J. *Surf. Sci.* **2007**, *601*, 5510–5514.

(26) Myrseth, V.; Bozek, J. D.; Kukk, E.; Sæthre, L. J.; Thomas, T. D. *J. Electron Spectrosc. Relat. Phenom.* **2002**, *122*, 57–63.

(27) Carroll, T. X.; Børve, K. J.; Sæthre, L. J.; Bozek, J. D.; Kukk, E.; Hahne, J. A.; Thomas, T. D. *J. Chem. Phys.* **2002**, *116*, 10221–10228.

(28) van der Straten, P.; Morgenstern, R.; Niehaus, A. *Z. Phys. D* **1988**, *8*, 35–45.

(29) Oltedal, V. M.; Børve, K. J.; Sæthre, L. J.; Thomas, T. D.; Bozek, J. D.; Kukk, E. *Phys. Chem. Chem. Phys.* **2004**, *6*, 4254–4259.

(30) Dunning, T. H., Jr. *J. Chem. Phys.* **1971**, *55*, 716–723.

(31) Krishnan, R.; Binkley, J. S.; Seeger, R.; Pople, J. A. *J. Chem. Phys.* **1980**, *72*, 650–654.

(32) McLean, A. D.; Chandler, G. S. *J. Chem. Phys.* **1980**, *72*, 5639–5648.

(33) Karlsen, T.; Børve, K. J.; Sæthre, L. J.; Wiesner, K.; Bässler, M.; Svensson, S. *J. Am. Chem. Soc.* **2002**, *124*, 7866–7873.

(34) Stevens, W. J.; Basch, H.; Krauss, M. *J. Chem. Phys.* **1984**, *81*, 6026–6033.

(35) Karlsen, T.; Børve, K. J. *J. Chem. Phys.* **2000**, *112*, 7979–7985.

(36) Frisch, M. J. *Gaussian 03*, revision C.02; Gaussian, Inc.: Wallingford, CT, 2004.

(37) Dunning, T. H., Jr. *J. Chem. Phys.* **1989**, *90*, 1007–1023.

(38) Kendall, R. A.; Dunning, T. H., Jr.; Harrison, R. J. *J. Chem. Phys.* **1992**, *96*, 6796–6806.

(39) Ren, P.; Ponder, J. W. *J. Phys. Chem. B* **2003**, *107*, 5933–5947.

(40) Ren, P.; Ponder, J. W. *J. Comput. Chem.* **2002**, *23*, 1497–1506.

(41) Ponder, J. W.; Richards, F. M. *J. Comput. Chem.* **1987**, *8*, 1016–1024.

(42) Abu-samha, M.; Børve, K. J.; Sæthre, L. J.; Öhrwall, G.; Bergersen, H.; Rander, T.; Björneholm, O.; Tchaplyguine, M. *Phys. Chem. Chem. Phys.* **2006**, *8*, 2473–2482.

(43) Carroll, T. X.; Berrah, N.; Bozek, J.; Hahne, J.; Kukk, E.; Sæthre, L. J.; Thomas, T. D. *Phys. Rev. A* **1999**, *59*, 3386–3393.

(44) Sundin, S.; Sæthre, L. J.; Sorensen, S. L.; Ausmees, A.; Svensson, S. *J. Chem. Phys.* **1999**, *110*, 5806–5813.

(45) McFeely, F. R.; Zhang, K. Z.; Banaszak Holl, M. M. *Mater. Res. Soc. Symp. Proc.* **1997**, *446*, 15–20.

(46) Sæthre, L. J.; Siggel, M. R. F.; Thomas, T. D. *J. Electron Spectrosc. Relat. Phenom.* **1989**, *49*, 119–137.

(47) Yaws, C. L. *Chemical properties handbook*; McGraw-Hill: New York, 1999; pp 189, 195, 241, and 247.
(48) Green, M.; Keevers, M. *Prog. Photovolt.* **1995**, *3*, 189–192.
(49) Weiss, K.; Ostrom, H.; Triguero, L.; Ogasawara, H.; Garnier, M. G.; Pettersson, L. G. M.; Nilsson, A. *J. Electron Spectrosc. Relat. Phenom.* **2003**, *128*, 179–191.
(50) Thomas, T. D. *J. Chem. Phys.* **1970**, *52*, 1373–1380.
(51) Holme, A.; Børve, K. J.; Sæthre, L. J.; Thomas, T. D. To be published.
(52) Myrseth, V.; Sæthre, L. J.; Børve, K. J.; Thomas, T. D. *J. Org. Chem.* **2007**, *72*, 5715–5723.
(53) Myrseth, V.; Børve, K. J.; Wiesner, K.; Bässler, M.; Svensson, S.; Sæthre, L. J. *Phys. Chem. Chem. Phys.* **2002**, *4*, 5937–5943.
(54) Sæthre, L. J.; Berrah, N.; Bozek, J. D.; Børve, K. J.; Carroll, T. X.; Kukk, E.; Gard, G. L.; Winter, R.; Thomas, T. D. *J. Am. Chem. Soc.* **2001**, *123*, 10729–10737.
(55) Holme, A.; Sæthre, L. J.; Børve, K. J.; Thomas, T. D. *J. Mol. Spectrosc.* **2009**, *920*, 387–392.
(56) Jean, Y.; Volatron, F.; Burdett, J. *An introduction to molecular orbitals*; Oxford University Press: New York, 1993; pp 258−267.
(57) Roy, K. K. *Potential Theory in Applied Geophysics*; Springer: Berlin, 2008; Chapter *7*, pp 151−205.
(58) Gradshteyn, I. S.; Ryzhik, I. M. *Tables of integrals, series and products*; Academic Press: New York, 1980.
(59) Kumagai, M.; Takagahara, T. *Phys. Rev. B* **1989**, *40*, 12359–12381.
(60) Makov, G.; Nitzan, A.; Brus, L. E. *J. Chem. Phys.* **1988**, *88*, 5076–5085.
(61) Makov, G.; Nitzan, A. *J. Phys. Chem.* **1994**, *98*, 3459–3466.
(62) Rotenberg, E.; Olmstead, M. A. *Phys. Rev. B* **1992**, *46*, 12884–12887.

JP1003352